

CGI-58 Is an α/β -Hydrolase within Lipid Transporting Lamellar Granules of Differentiated Keratinocytes

Masashi Akiyama,* Kaori Sakai,*
Chitoshi Takayama,[†] Teruki Yanagi,*
Yasuko Yamanaka,* James R. McMillan,*
and Hiroshi Shimizu*

From the Department of Dermatology,* Hokkaido University Graduate School of Medicine, Sapporo, Japan; Department of Molecular Anatomy,[†] University of the Ryukyus School of Medicine, Okinawa, Japan

CGI-58 is the causative molecule underlying Dorfman-Chanarin syndrome, a neutral lipid storage disease exhibiting apparent clinical features of ichthyosis. CGI-58, associated with triacylglycerol hydrolysis, has an α/β -hydrolase fold and is also known as the α/β -hydrolase domain-containing protein 5. The purpose of this study was to elucidate the function of CGI-58 and the pathogenic mechanisms of ichthyosis in Dorfman-Chanarin syndrome. Using an anti-CGI-58 antibody, we found CGI-58 to be expressed in the upper epidermis, predominantly in the granular layer cells, as well as in neurons and hepatocytes. Immunoelectron microscopy revealed that CGI-58 was also localized to the lamellar granules (LGs), which are lipid transport and secretion granules found in keratinocytes. CGI-58 expression was markedly reduced in the epidermis of patients with harlequin ichthyosis, demonstrating defective LG formation. In cultured keratinocytes, CGI-58 expression was mildly up-regulated under high Ca^{2+} conditions and markedly up-regulated in three-dimensional, organotypic cultures. In the developing human epidermis, CGI-58 immunostaining was observed at an estimated gestational age of 49 days, and CGI-58 mRNA expression was up-regulated concomitantly with both epidermal stratification and keratinocyte differentiation. CGI-58 knockdown reduced expression of keratinocyte differentiation/keratinization markers in cultured human keratinocytes. Our results indicate that CGI-58 is expressed and packaged into LGs during keratinization and likely plays crucial role(s) in keratinocyte differentiation and LG lipid metabolism, contributing to skin lipid barrier formation. (*Am J Pathol* 2008, 173:1349–1360; DOI: 10.2353/ajpath.2008.080005)

CGI-58 (*ABHD5*) is one of the genes that has been identified using the comparative proteomic approaches between *Caenorhabditis elegans* and humans.¹ CGI was named after comparative gene identification. CGI-58 (α/β -hydrolase domain-containing protein 5; ABHD5) is a member of α/β -hydrolase family and a putative esterase/lipase/thioesterase. The physiological roles of CGI-58 protein were reported to be lipolytic degradation of fat in the lipid storing cells.² However, its roles in various tissues including the epidermis have not yet been clarified.¹ In 2001, CGI-58 mutations were identified in Dorfman-Chanarin syndrome (DCS; MIM 275630) families from the Mediterranean region³ and, later, in a DCS patient of Japanese origin.⁴ Additional DCS cases with CGI-58 mutations have been reported.^{5–7}

DCS is an autosomal recessively inherited neutral lipid storage disease and is characterized by ichthyosis.^{8,9} This entity shows leukocyte lipid vacuoles and involvement of several internal organs, including liver dysfunction, myopathy, cataracts, and a variety of neurological symptoms. The most characteristic feature of DCS is ragged skin over the entire body, caused by thickening of the cornified layers of skin surface, termed ichthyosis. All DCS cases present with this skin manifestation, ie, moderate to severe non-bullous congenital ichthyosiform erythroderma.^{10,11}

It was reported that truncation of CGI-58 protein results in abnormal lamellar granule (LG) formation in DCS.⁴ LGs have been shown to form a continuous network from the Golgi apparatus (trans-Golgi network; TGN). LGs are multifunctional and are involved in packaging and secretion of a variety of enzymes and structural proteins. LGs are known to be involved in lipid transport and secretion in keratinocytes and are thought to play a crucial role in epidermal lipid barrier formation.¹²

To date, the function of CGI-58 in the skin, the liver and the brain has not been clarified and the exact mechanism of pathogenesis of ichthyosis, liver dysfunction and men-

Supported in part by Grant-in-Aid from the Ministry of Education, Science, Sports, and Culture of Japan to Masashi Akiyama (Kiban B 18390310 and Kiban B 20390304).

Accepted for publication July 31, 2008.

Address reprint requests Masashi Akiyama, M.D., Ph.D., Department of Dermatology, Hokkaido University Graduate School of Medicine, N15 W7, Sapporo 060-8638, Japan, E-mail: akiyama@med.hokudai.ac.jp.

tal retardation in DCS is not well understood. In this study, to elucidate the function of CGI-58 in the skin and to better understand the pathogenic mechanisms underlying the DCS phenotype including the ichthyosis, the expression patterns of CGI-58 were examined in normal human skin, harlequin ichthyosis patients' LG deficient skin, developing human fetal epidermis *in vivo* and cultured human keratinocytes *in vitro*. In addition, CGI-58 expression was studied in mouse organs including the skin. Our findings clearly demonstrated for the first time that CGI-58 is expressed in the upper epidermis, predominantly in the granular layer cells, as well as in neurons and hepatocytes. Immunoelectron microscopy revealed that CGI-58 is localized to the LGs, which are lipid transporting and secreting granules in keratinocytes. CGI-58 expression was up-regulated during keratinocyte differentiation (keratinization) and human skin development. Reduced expression of keratinocyte differentiation markers was seen in CGI-58 knockdown keratinocytes. These facts suggest that CGI-58 plays crucial role(s) in epidermal keratinocyte differentiation and keratinocyte LG lipid metabolism, contributing to the skin lipid barrier formation.

Materials and Methods

Production of Anti-CGI-58 Antibody

Polyclonal anti-CGI-58 antibody was raised in rabbits using a 14 amino acid sequence synthetic peptide (residues 181-194) derived from the CGI-58 sequence (AL606838) as the immunogen (Sigma Genosys, Hokkaido, Japan). Rabbits were immunized by antigen injection (every 2 weeks, total six times). During the immunization period, serum anti-CGI-58 antibody titers were checked by enzyme-linked immunosorbent assay three times to confirm antibody production. At 77 days after the first antigen injection, the rabbits were sacrificed and entire serum was obtained. Anti-CGI-58 antisera were subsequently purified using an antigen affinity column. Immunofluorescent and immunohistochemical staining confirmed that the anti-CGI-58 antisera worked on frozen tissue sections. However, we could not obtain consistent staining results with the anti-CGI-58 antibody on routine, formalin-fixed and paraffin-embedded tissue sections.

Human Fetal and Adult Skin Specimens

Normal human fetal tissue was acquired (after informed consent was obtained) from Sapporo Maternity-Women's Hospital (Sapporo, Japan). Human embryonic and fetal skin specimens were obtained from abortuses of 79 to 135 days estimated gestational age (EGA). Skin specimens were taken from the trunk, scalp, and fingers, and processed for the present study. EGA was determined from maternal history, fetal measurements (crown rump and foot length) and comparative histological appearance of the epidermis.

Normal adult human skin samples were obtained at surgical operations of benign subcutaneous tumors under fully informed consent at the Department of Der-

matology, Hokkaido University Graduate School of Medicine.

Ichthyosis Patients with LG Abnormalities

DCS Patient Harboring a CGI-58 Truncation Mutation

The patient had presented with severe ichthyosis since birth. The detailed information on this patient was previously described.⁴ He had demonstrated liver dysfunction since infancy and a liver biopsy showed cirrhosis with severe fatty degeneration. He also had slight mental retardation. White blood cells in the peripheral blood and the basal cells and the lowermost spinous cells of the epidermis demonstrated large cytoplasmic lipid vacuoles characteristic of DCS. The patient was a homozygote for a nonsense mutation 550C>T transition (c.550C>T) in exon 4 of CGI-58 [sequence according to Lefèvre et al³] (GenBank accession No. AL606839) that changed an arginine residue to a stop codon (p.Arg184X).⁴

Harlequin Ichthyosis Patients Harboring ABCA12 Mutations

Both harlequin ichthyosis patients showed typical clinical features including thick scales over their entire body surface, severe ectropion, eclabium, and malformed pinnae. Both patients were homozygotes for ABCA12 truncation mutations and these mutations were predicted to lead to severe defects in ABCA12 keratinocyte lipid transporter function. The details of the harlequin ichthyosis patients were reported previously.¹³

Human Liver and Brain Samples

Frozen tissue slides of human liver and brain were purchased from BioChain Institute Inc. (Hayward, CA). Normal human adult liver or brain tissue sections cut at 5 to 10 μ m thickness were mounted on a positively charged glass slide. The slides were fixed and dehydrated with acetone.

Mice

C57BL/6J mice were purchased from Clea Japan Inc. (Tokyo, Japan). The mice were kept in isolator cages in a barrier facility under a 12 hours light cycle and maintained under specific pathogen-free conditions.

Cell Culture

Neonatal human keratinocytes were purchased from Cambrex BioScience Walkersville, Inc. (Walkersville, MD). Human keratinocytes were cultured in Defined keratinocyte serum-free medium (Invitrogen, San Diego, CA). The keratinocytes were cultured in low Ca²⁺ conditions (0.09 mmol/L) to maintain a basal cell-like population of undifferentiated cells. To induce terminal differentiation, CaCl₂ was added directly to the culture media for a final 2 mmol/L calcium concentration. In addition, three-

dimensional, organotypic cultured epidermal sheets cultured over a non-proliferative fibroblast feeder layer (Japan Tissue Engineering Co. J-TEC, Aichi, Japan) were used for the study.

Antibodies

Primary antibodies to keratinization-associated proteins used in the present study were rabbit polyclonal anti-involucrin antibody (Biomedical Technologies, Inc., Stoughton, MA), mouse monoclonal anti-loricrin antibody (Covance Lab., Richmond, CA), and mouse monoclonal anti-transglutaminase 1 antibody (Biomedical Technologies, Inc., Stoughton, MA). As markers for TGN and LG contents, a TGN-marker; sheep polyclonal anti-TGN-46 antibody (Serotec Inc., Oxford, UK), anti-LG content antibodies; rabbit anti-human cathepsin D antibody (Santa Cruz Biotechnology, Inc., CA), and rabbit polyclonal anti-human β defensin 3 antibody (Novus Biologicals, Littleton, CO). Human β defensin 3 was reported to be localized to LGs.¹⁴

In addition, rabbit polyclonal anti-glucosylceramide antibody (Glycobiotech, Kuekel, Germany) was used in the present study.

Immunoblotting

Cell lysates were prepared by homogenization in lysis buffer (50 mmol/L Tris-HCl [pH 7.6], 150 mmol/L NaCl, 1% NP-40, 0.1% SDS, 0.25% sodium deoxycholate), followed by centrifugation at 15000 rpm for 5 minutes. In addition, normal mouse and human tissue extracts were purchased from BioChain Institute, Inc. (Hayward, CA). Cell lysates (100 μ g of protein per lane) were resolved on 12.5% SDS-polyacrylamide gels that were then electroblotted onto Immobilon-P membranes (Millipore, Bedford, MA) using a wet transfer apparatus. Membranes were probed with the rabbit polyclonal anti-CGI-58 antiserum (final dilution 1:10). Proteins were detected with horseradish peroxidase-conjugated secondary antibodies (Jackson ImmunoResearch Laboratory, West Grove, PA), and specific bands were visualized by chemiluminescence.

Real-Time Reverse Transcription-Polymerase Chain Reaction Analysis

To quantify the CGI-58 mRNA expression levels, total RNA was extracted from human keratinocytes cultured in low Ca^{2+} or high Ca^{2+} condition, and extracted from human adult and fetal skin. RNA samples were analyzed by ABI prism 7000 sequence detection system (Applied Biosystems, Lincoln Centre Drive Foster City, CA). Probes for real-time RT-PCR were as follows: a probe for CGI-58, Applied Biosystems, ID Hs 00211205_m1; a probe for involucrin, Applied Biosystems, ID Hs 00846307_sl; a probe for loricrin, Applied Biosystems, ID Hs 01894962_sl; a probe for transglutaminase 1, Applied Biosystems, ID Hs 00165929_ml; a probe for filaggrin, Applied Biosys-

tems, ID Hs 00863478_gl. Differences between the mean CT values of CGI-58 and that of glyceraldehyde-3-phosphate dehydrogenase (GAPDH) were calculated as $\Delta\text{CT}_{\text{sample}} = \text{CT}_{\text{CGI-58}} - \text{CT}_{\text{GAPDH}}$ and those of CT for the normal adult skin as $\Delta\text{CT}_{\text{calibrator}} = \text{CT}_{\text{CGI-58}} - \text{CT}_{\text{GAPDH}}$.

RNA Interference and Generation of Lentiviruses

CGI-58 expression was depleted using short interfering RNA duplexes. Target regions in CGI-58 were identified by the BLOCK-iT RNA interference (RNAi) Designer Program (Invitrogen, San Diego, CA). Two sequences were used to generate RNAi molecules that target either 498-518 coding region of CGI-58 gene (RNAi 498, sequence 5'-CAGTTTGTGGAATCCATTGAA-3'; CGI-58 #1) or to the 886-906 region (RNAi 886, sequence 5'-GTGAGACAGCTTCAAGAATA-3'; CGI-58 #2). These sequences were synthesized as DNA oligonucleotides and in addition contained complementary sequences joined by a 5'-GTTTTGGCCACTGACTGAC-3' loop. Synthetic duplexes were cloned into the pcDNA6.2GW/Em green fluorescent protein (GFP) vector in the middle of the microRNA155 (miR155) sequence supplied as a part of the BLOCK-iT Lentiviral Pol II miR RNA expression system kit (Invitrogen, San Diego, CA). In the pcDNA6.2GW/EmGFP vector the chimeric miR155-CGI-58 sequence is located under the control of the cytomegalovirus promoter co-cis-translationally with EmGFP. On processing in the cells by the endogenous endonuclease machinery, the construct produces anti-CGI-58 RNA duplex (microRNA [miRNA]-CGI-58 #1 and #2). We used the control vector pcDNA6.2GW/EmGFP-miR-neg that encodes random mRNA that fails to target any known vertebrate gene (scrambled control miRNA, Invitrogen, San Diego, CA). The expression cassette was transferred to the lentiviral shuttle vector pLenti6/V5-DEST vector (Invitrogen, San Diego, CA) by Gateway recombination following the instructions. For the generation of infectious lentiviral particles pLenti6/V5-DEST vectors containing miRNA-CGI-58 or miR-neg cassettes were co-transfected with ViraPower packaging plasmid mixture: pLP1, pLP2, and pLP/VSV-G (Invitrogen) into 293FT cells using Lipofectamine 2000 (Invitrogen). Ten-cm tissue culture plates were used to produce each batch of lentivirus. Virus-containing media was collected 60 hours after transfection, centrifuged at 2000 rpm for 20 minutes and filtered through a 0.45 μ m filter (Millipore). Transduction of miRNA viruses to normal human keratinocytes was conducted following the manufacturer's protocol. Briefly, normal human keratinocytes in 6-well plates were infected by 2-ml supernatants in the presence of 6 μ g/ml Polybrene (Invitrogen). Six hours later, we removed the medium containing virus and replaced it with KGM-2 culture medium. After switching to high Ca^{2+} culture conditions, expression of CGI-58 and keratinocyte differentiation markers including involucrin, loricrin, filaggrin, and transglutaminase 1 was studied by real-time PCR analysis.

Immunofluorescent Labeling

The tissue samples or three-dimensional, organotypic cultured epidermal sheets were immediately frozen in optimal cutting temperature compound (Tissue-Tek; Sakura Finetechnical, Tokyo, Japan), and cut at a thickness of 6 μm . Immunofluorescent labeling was performed as previously described.¹⁵ Briefly, 6- μm thick sections of fresh tissue samples cut using a cryostat or cultured cells were prepared for immunolabeling. Sections were fixed in acetone for 10 minutes at room temperature for labeling with anti-human CGI-58 antibody or other antibodies. The sections were incubated in primary antibody solution for 2 hours at room temperature. Primary antibodies and dilutions were as follows; rabbit polyclonal anti-human CGI-58 antibody, 1/10; mouse monoclonal anti-cathepsin D antibody, 1/10; rabbit polyclonal anti-human β -defensin 3 antibody, 1/250; sheep polyclonal anti-TGN-46 antibody, 1/4; rabbit polyclonal anti-involucrin antibody, neat; mouse monoclonal anti-loricrin antibody, 1/250; and mouse monoclonal anti-transglutaminase 1 antibody, 1/10. The sections were then incubated in fluorescein isothiocyanate (FITC)-conjugated rabbit anti-mouse immunoglobulin (Jackson ImmunoResearch Laboratories, Inc. West Grove, PA) or donkey anti-rabbit immunoglobulins (DAKO, Glostrup, Denmark) diluted 1:100 for 2 hours at room temperature, followed by 10 $\mu\text{g/ml}$ TOPRO3 (Sigma Chemical Co., St. Louis, MO) to counterstain nuclei for 10 minutes at 37°C or 10 $\mu\text{g/ml}$ propidium iodide for 10 seconds. Sections were observed under an Olympus Fluoview confocal laser scanning microscope (Olympus, Tokyo, Japan). Furthermore, cultured cells were stained with similar procedures.

Immunohistochemistry on Mice Tissues

Under deep ether anesthesia, 1-month-old mice (C57Bl/6CrSlc) were fixed by transcardial perfusion with 4% paraformaldehyde in a phosphate buffer (0.1M, pH 7.4). The brains and livers were immersed in the same fixative overnight, cryoprotected with 30% sucrose in phosphate buffer for 2 days at 4°C, and then cut into coronal sections at a thickness of 20 μm with a cryostat. The sections, mounted on gelatin-coated glass slides were treated as follows; with methanol containing 0.3% H_2O_2 for 30 minutes, pepsin solution (1 $\mu\text{g/ml}$ in 0.2N HCl) for 5 minutes at 37°C, phosphate buffer for 10 minutes, 3% normal goat serum in phosphate buffer for 1 hour, and a rabbit anti-CGI-58 antibody (diluted 1:500) for 2 days at 4°C. After rinsing three times with phosphate buffer for 15 minutes, sections were visualized using the avidin-biotin-peroxidase complex method. After finishing diaminobenzidine reaction, sections of brain and liver were stained with Toluidine blue and hematoxylin, respectively.

Postembedding Immunoelectron Microscopy

Normal human skin samples were obtained from surgical operations of benign subcutaneous skin tumors under

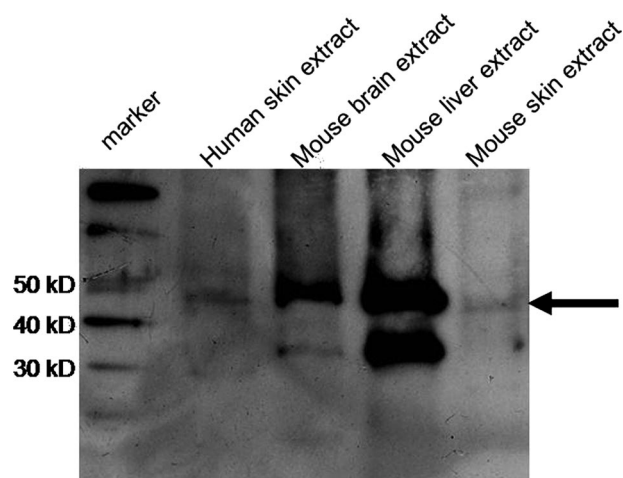


Figure 1. Immunoblot Analysis with Anti-CGI-58 Antiserum. Immunoblot analysis with the anti-CGI-58 antiserum using total protein samples extracted from normal human skin, mouse brain, mouse liver, and mouse skin. An approximate 45 kDa band (arrow) was detected by the antiserum in extracts from normal human skin, mouse brain, mouse liver and mouse skin (from the second left to right). The left is a marker lane.

fully informed consent, and were processed for postembedding immunoelectron microscopy as previously described.¹³ Cyrofixed cryosubstituted samples were embedded in Lowicryl K11M resin. Ultrathin sections were cut and incubated with anti-CGI-58 antisera antibody, a secondary linker antibody, and a 5-nm gold-conjugated antibody for immunogold labeling.

Results

Establishment of Anti-CGI-58 Antibody

Immunoreactivity of the antiserum to the synthetic peptide (residue 181-194 of CGI-58) was confirmed by enzyme-linked immunosorbent assay with the synthetic peptide (data not shown). By immunoblot analysis, anti-CGI-58 antiserum exhibited approximately 45-kDa bands both in the human skin and the mouse skin extracts (Figure 1).

CGI-58 Expression in the Brain and the Liver

DCS patients with CGI-58 deficiency show neurological and hepatic symptoms including mental retardation, liver dysfunction, and liver cirrhosis. Thus, using the anti-CGI-58 antisera that we have created CGI-58 localization in the brain and the liver was studied.

By immunoblot analysis, approximately 45 kDa-bands representing the CGI-58 peptide were detected in extracts from mouse brain and liver (Figure 1).

Strong CGI-58-immunolabeling was observed in the brain and liver of mice (Figure 2). In the brain, CGI-58-containing cells were confined within the hypothalamus (arrows in Figure 2A), and no labeled cells were detected in other areas, such as the cerebral cortex, hippocampus, thalamus, brain stem, cerebellum, and spinal cord. In the hypothalamus, CGI-58 was localized in medium-

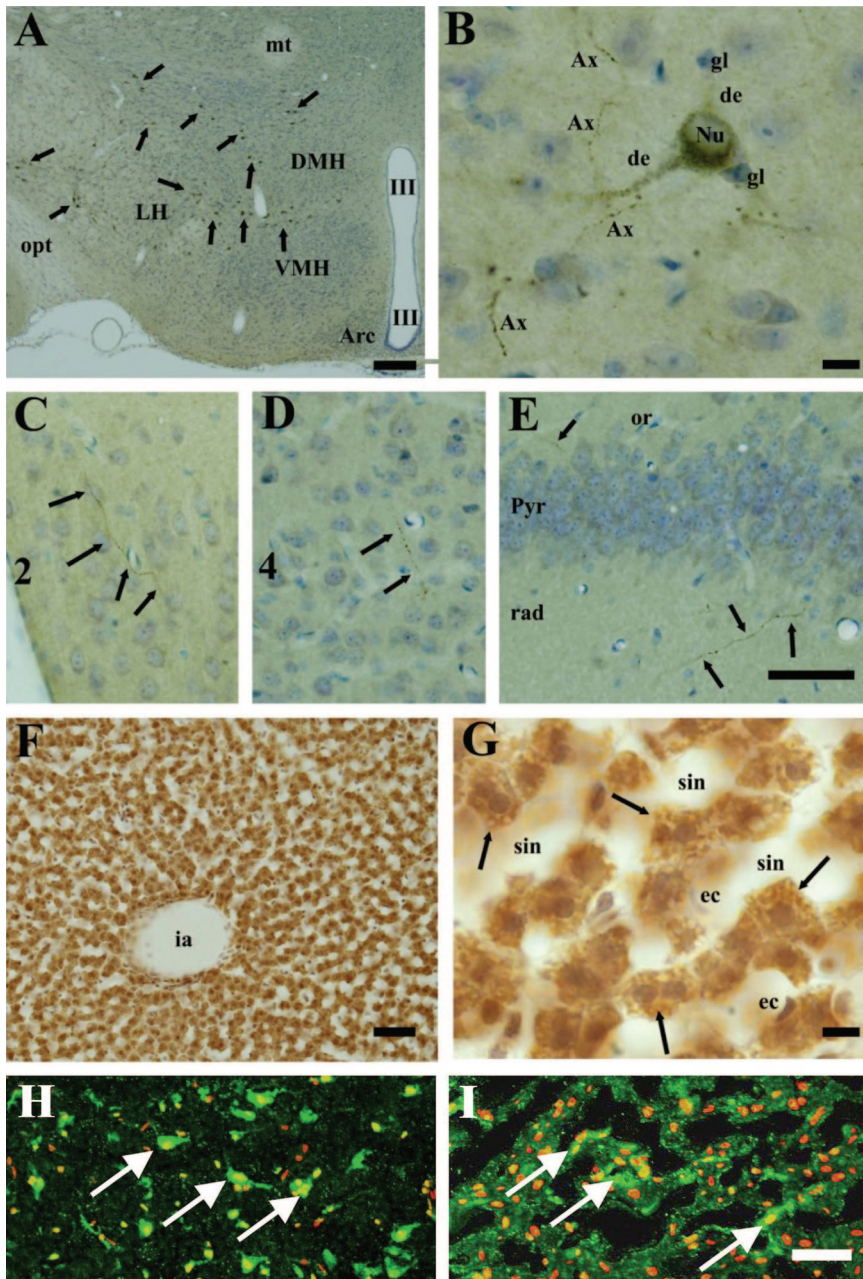


Figure 2. CGI-58 Distribution in the Brain and the Liver. Immunohistochemical localization of CGI-58 in the mouse brain (A–E) and liver (F, G). **A–D:** Hypothalamus at lower magnification (A) and at higher magnification (B–E). **A:** CGI-58-positive neurons (arrows) scattered in the hypothalamus. **B:** CGI-58-immunolabeling exhibited quite fine granules in the dendrites (de) and perikarya, but nuclei (Nu) were negative. Small neurons and glial cells (gl) did not contain CGI-58. Axons (Ax) with varicosities were densely stained. **C–E:** CGI-58-positive axons (arrows) entered into the layer 2 (C) and layer 4 (D) of the somatosensory cortex, oriens layer (or) and stratum radiatum (rad) of hippocampal formation CA1 region (E). These axons were also detected within the pyramidal cell layer of hippocampus (Pyr). **F, G:** The liver at lower magnification (F) and at higher magnification (G). Hepatocytes abundantly expressed the CGI-58. The CGI-58-immunolabeling exhibited a fine granular pattern in the cytosol (arrows). **H, I:** CGI-58 distribution in the human brain (H) and liver (I). In the normal human brain, CGI-58-positive neurons (white arrows) were scattered (H). In the normal human liver, cytoplasmic CGI-58 staining (white arrows) was seen in the hepatocytes (I). Abbreviations: Arc; arcuate hypothalamic nucleus, DMH; dorsomedial hypothalamic nucleus, ec; endothelial cells, ia; interlobular artery, LH; lateral hypothalamic area, mt; mammillothalamic tract, opt; optic tract, sin; sinusoid, III; third ventricle, VMH; ventromedial hypothalamic nucleus. CGI-58, green (FITC); nuclear stain, red (propidium iodide). Scale bars = 50 μm.

sized (diameter ~15 to 30 μm) multipolar neurons. The stained neurons were scattered throughout the hypothalamus, but did not accumulate in specific nuclei, such as the dorsomedial hypothalamic nucleus, ventromedial hypothalamic nucleus complex, arcuate hypothalamic nucleus. In higher magnification pictures of the hypothalamus, CGI-58-immunolabeling exhibited quite a fine granular pattern in the perikarya, dendrites and axons of neurons, but glial cells and blood vessel endothelial cells were negative (Figure 2B). Furthermore, CGI-58-containing axons extended into the cerebral cortex (Figure 2, C and D) and hippocampus (Figure 2E).

In the liver, CGI-58 was abundantly expressed in hepatocytes, but the sinusoidal endothelial cells and blood cells were negative (Figure 2, F and G). In the

hepatocytes, CGI-58-immunolabeling exhibited a fine granular pattern (arrows), occupying the cytosol.

The corneal epithelium was only weakly labeled with anti-CGI-58 antisera (data not shown), and CGI-58 was not detected in the epithelia of the digestive organs or the urogenital organs.

Immunofluorescent localization of CGI-58 revealed that human liver hepatocytes and brain neurons showed discrete cytoplasmic labeling (Figure 2, H and I).

CGI-58 Distribution in the Epidermis

Congenital ichthyosiform erythroderma on the whole body surface is one of the major symptoms of DCS

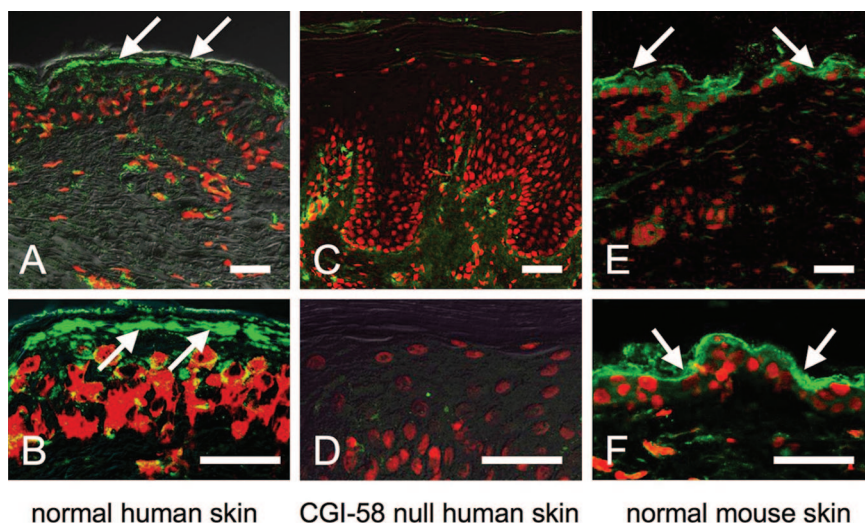


Figure 3. CGI-58 Distribution in the Skin. **A, B:** Immunoreactivity of the anti-CGI-58 antiserum in normal human skin. CGI-58 immunolabeling (green, FITC) was seen in the epidermis, predominantly in the granular layer (**arrows**) and in the dermal fibroblasts in human skin. **C, D:** Anti-CGI-58 antiserum showed no labeling in CGI-58 null epidermis of a DCS patient with homozygous CGI-58 truncation mutation (Akiyama et al.⁴). **E, F:** CGI-58 distribution in murine skin. CGI-58 labeling (Green, FITC) was also observed in the epidermis and fibroblasts of mouse skin. CGI-58, green (FITC); nuclear stain, red (propidium iodide). Scale bars = 50 μ m.

caused by CGI-58 deficiency. Thus, we studied the distribution of CGI-58 in the epidermis to obtain clues to clarify the function of CGI-58 and the pathomechanisms of ichthyosis in DCS.

In normal human skin, the anti-CGI-58 antiserum stained the upper epidermal layers, mainly the granular layers in addition to dermal fibroblasts (Figure 3, A and B), although no apparent CGI-58-positive neurons in dermal nerves were observed. In contrast, there was an absence of immunolabeling in the skin of our DCS patient, who harbors a homozygous truncation mutation p.Arg184X⁴ (Figure 3, C and D). This mutation resulted in truncation of the protein, leading to loss of epitope expression, ablating CGI-58 antiserum staining. These findings confirmed specificity of the anti-CGI-58 antibody.

In the skin of mice, CGI-58 immunoreactivity was seen in the upper epidermis and the dermal fibroblasts (Figure 3, E and F). This distribution pattern was similar to that of human skin.

Localization of CGI-58 to LGs of Differentiating Keratinocytes in Human Epidermis

To understand the function of CGI-58 in the epidermis, we investigated the ultrastructural localization of CGI-58 in keratinocytes.

Immunoelectron microscopy using cryofixed, cryosubstituted normal human skin samples revealed that CGI-58 protein was restricted to LGs in the cytoplasm of keratinocytes in the upper spinous and granular layers of epidermis (Figure 4A). In the granular layer cells, CGI-58-positive LGs were abundant in the cytoplasm (Figure 4B). High power views demonstrated that CGI-58 localized to the lamellar structures in LGs (Figure 4, C and D). CGI-58-positive LGs were observed fusing with the cell membrane to secrete their content into the extracellular space of the stratum corneum (Figure 4A). CGI-58 immunogold-labeling was sparsely distributed in the cytoplasm of

fibroblasts and exhibited no restricted localization to any specific organelle (data not shown).

Reduced Expression of CGI-58 in LG-Deficient Harlequin Ichthyosis Skin

To confirm the localization of CGI-58 in LGs, we performed CGI-58 immunostaining in LG deficient harlequin ichthyosis epidermis.

In harlequin ichthyosis patient epidermis, normal LGs are absent and only lipid droplets and defective LGs lacking lipid contents due to loss of function of the *ABCA12* transporter are seen. In such harlequin ichthyosis epidermis, remarkably reduced immunolabeling for CGI-58 was observed (Figure 5, A and B), compared with that observed in normal human skin (Figure 5C). These

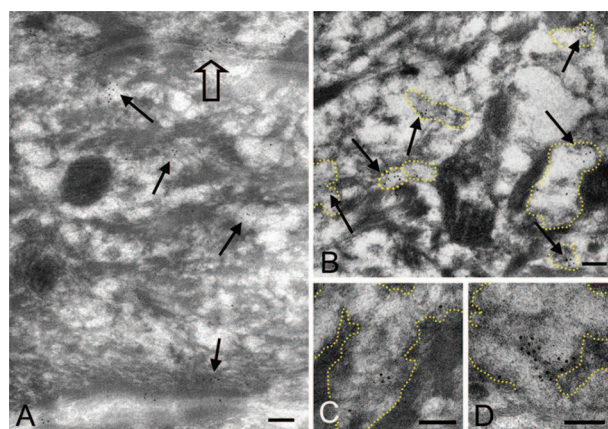


Figure 4. Cryosubstituted, Cryofixed Postembedding Immunoelectron Microscopy with Anti-CGI-58 Antiserum in Normal Human Epidermis. **A:** Anti-CGI-58 antibody deposition labeled with 5 nm gold particles was seen on cytoplasmic vesicles (**arrows**) in the uppermost spinous and granular layer keratinocytes. CGI-58 was secreted with lamellar content of a vesicle to the intercellular space (**open arrow**). **B:** CGI-58-positive granules (**arrows**) contained lamellar structures inside and were identified as LGs. **C, D:** CGI-58 labeling was observed on the lamellar structure of LGs. Margin of LGs is traced with yellow dots. Scale bars = 100 nm (**A–D**).

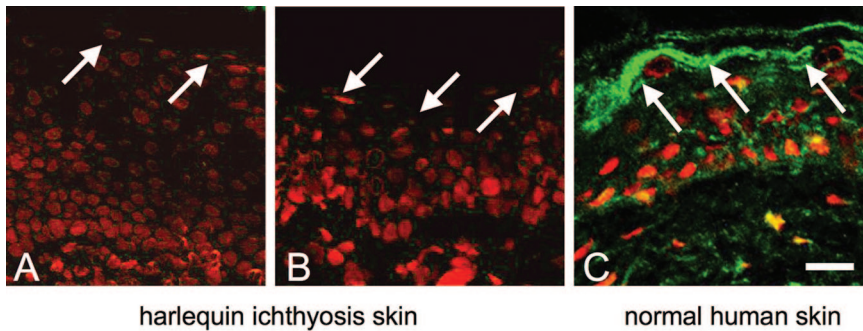


Figure 5. CGI-58 Immunolabeling in Harlequin Ichthyosis Patients' Epidermis. In skin specimens from the two harlequin ichthyosis patients with defective LGs (**A, B**), extremely reduced CGI-58 expression was seen compared with strong CGI-58 staining in normal human skin (**C**). CGI-58, green (FITC); nuclear stain, red (propidium iodide). **White arrows**, the granular layer. Scale bars = 50 μm .

findings indicated that CGI-58 is associated with LGs in the epidermis.

Preserved TGN-LG System in CGI-58 Null Human Epidermis

LGs are known to be multifunctional and they transport and secrete a variety of molecules other than lipids. To clarify whether CGI-58 in LGs is associated mainly with LG lipid contents or alternatively associated with non-lipid molecules, we studied the distribution patterns of non-lipid contents of LGs and a TGN marker.

Immunofluorescent staining for the TGN marker TGN-46 and LG contents, cathepsin D and human β defensin 3, in CGI-58 null human epidermis (the DCS patient's epidermis) revealed that there was no remarkable difference in the expression of any of the three molecules (TGN-46, cathepsin D, and human β defensin 3) in the upper epidermis compared to normal control human skin (data not shown). These results suggested that CGI-58 in LGs was not directly associated with either the lipid contents or TGN system.

CGI-58 Expression Was Up-Regulated in Accordance with Keratinocyte Differentiation (Keratinization)

From the present results described above, CGI-58 localization in LGs was demonstrated and a role for CGI-58 in lipid transport/metabolism was therefore suggested in the epidermis. Lipid transport and secretion by LGs are important for skin lipid barrier formation during keratinization (keratinocyte differentiation). Thus, we investigated effects of keratinocyte differentiation and epidermal development on CGI-58 expression *in vivo* and *in vitro*.

Up-Regulation of CGI-58 Expression in Cultured Keratinocytes after Differentiation

Evaluation of the CGI-58 transcript population against the GAPDH transcript using real-time RT-PCR revealed that CGI-58 transcription was up-regulated 2.3-fold after 1 week in high Ca^{2+} culture compared with CGI-58 expression in keratinocytes cultured in low Ca^{2+} concentration (Figure 6A). Furthermore, CGI-58 expression was dramatically up-regulated in more advanced differentiation

cultures; CGI-58 expression was up-regulated 33-fold in the three-dimensional, organotypic keratinocyte cultures compared to CGI-58 expression of low Ca^{2+} condition cultures and up-regulated 16-fold compared to that of cultures in the simple high Ca^{2+} condition (Figure 6A).

As controls, expression of other keratinization-related molecules, including involucrin, loricrin and transglutaminase 1, were also studied and the mRNA expression of involucrin, loricrin and transglutaminase 1 was up-regulated 1.3-, 2.3-, and 1.6-fold after 1 week in high- Ca^{2+} culture, respectively. In the organotypic cultures, expression of involucrin was also up-regulated 27-fold compared to that of low Ca^{2+} condition cultures and 21-fold compared to that of high Ca^{2+} culture condition. Expression of transglutaminase 1 was up-regulated 3.6-fold and 2.3-fold compared to those of low Ca^{2+} condition and high Ca^{2+} condition, respectively. Strong loricrin expression was obtained in the organotypic cultures, although loricrin expression was very weak in the simple cultures.

Immunofluorescent staining for CGI-58 confirmed that differentiated (partially keratinized) keratinocytes cultured in high Ca^{2+} condition showed stronger CGI-58 staining than that in undifferentiated keratinocytes under low Ca^{2+} culture conditions (Figure 6, B and F). The organotypic cultures of keratinocytes showed highly differentiated features with keratinization similar to normal human epidermis (Figure 6J). In the organotypic cultures, CGI-58 protein expression was observed in all of the suprabasal keratinocyte layers (Figure 6K). Involucrin and transglutaminase 1, the control keratinization markers, exhibited stronger staining in differentiating keratinocytes cultured under high Ca^{2+} conditions than undifferentiated keratinocytes cultured in low Ca^{2+} conditions (Figure 6, C, E, G, I). Loricrin immunostaining was almost negative both in differentiating keratinocytes in high Ca^{2+} conditions and undifferentiated keratinocytes cultured in low Ca^{2+} conditions (Figure 6, D and H). In the organotypic cultures, involucrin and transglutaminase 1 proteins were distributed in all of the suprabasal layers of keratinocytes (Figure 6, L and N). Loricrin protein was seen only in the upper layers (Figure 6M). These results clearly indicated that CGI-58 expression in the keratinocytes is up-regulated by keratinocyte differentiation (keratinization).

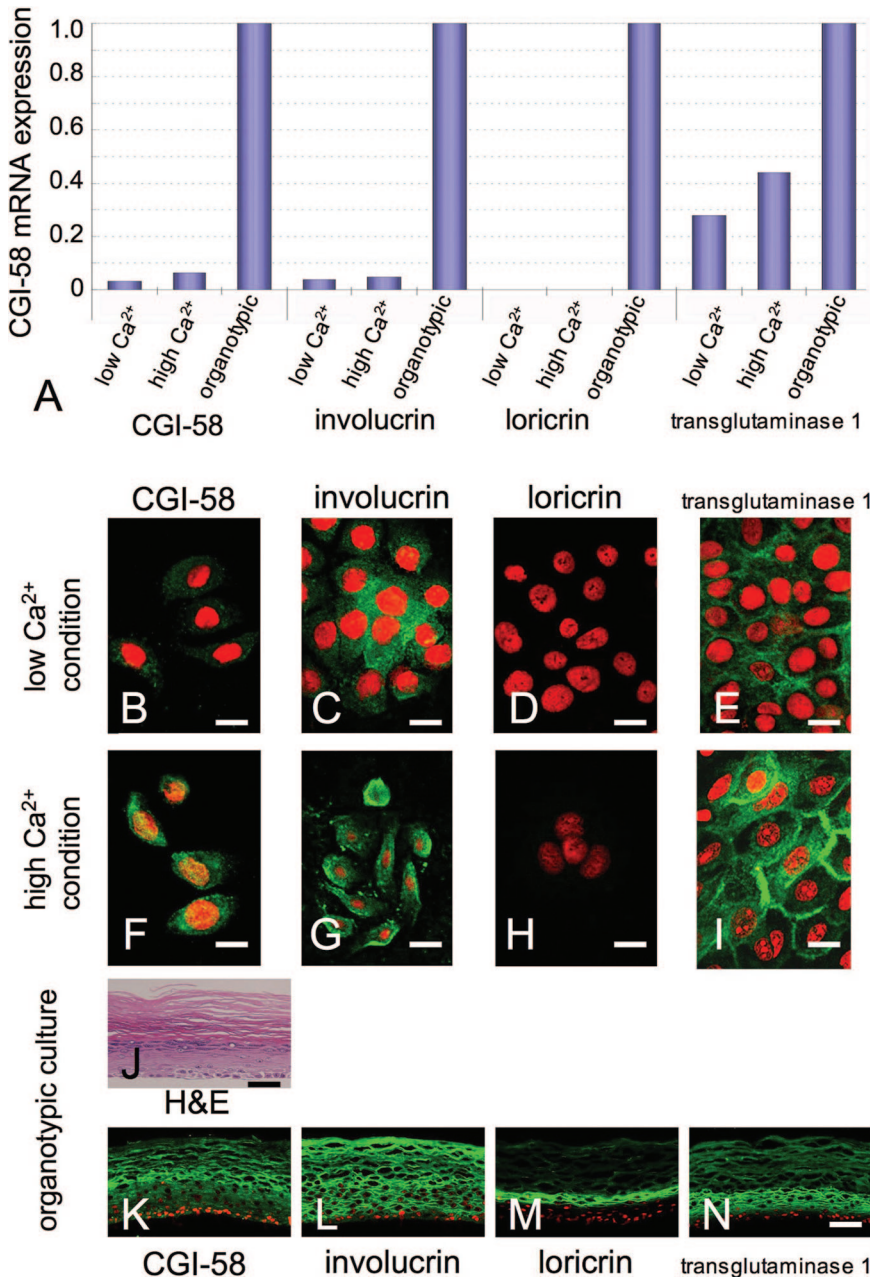


Figure 6. CGI-58 Expression during Human Keratinocyte Differentiation. **A:** Real-time RT-PCR analysis revealed that CGI-58 mRNA expression in human keratinocytes cultured in the high Ca²⁺ condition was 2.3-fold higher than that of cultured keratinocytes in low Ca²⁺ condition. CGI-58 expression in the organotypic cultures was up-regulated 33-fold compared to expression in low Ca²⁺ conditions. Expression of keratinization markers, involucrin, loricrin and transglutaminase 1, was also up-regulated in the three-dimensional, organotypic culture. **B–I:** Immunolabeling of normal cultured human epidermal keratinocytes. CGI-58 immunolabeling (FITC, green) was weak in the normal human keratinocytes cultured in low Ca²⁺ condition (**B**). In contrast, strong CGI-58 immunostaining was diffusely observed in the cytoplasm of normal human keratinocytes cultured in high Ca²⁺ condition (**F**). A weaker involucrin immunolabeling was seen in the normal human keratinocytes cultured in low Ca²⁺ condition (**C**) and strong involucrin immunostaining was diffusely observed in the cytoplasm of normal human keratinocytes cultured in high Ca²⁺ condition (**G**). No apparent loricrin immunostaining was observed either in the normal human keratinocytes cultured in low Ca²⁺ condition (**D**) or in the normal human keratinocytes cultured in high Ca²⁺ condition (**H**). Transglutaminase 1 immunolabeling was weak in the normal human keratinocytes cultured in low Ca²⁺ condition (**E**). Strong membranous transglutaminase 1 immunostaining was observed in the normal human keratinocytes cultured in high Ca²⁺ condition (**I**). **J:** Organotypic cultured, epidermal sheets stained with H&E showed highly differentiated specific features of keratinization, similar to that seen in normal skin. **K–N:** The suprabasal layers of organotypic keratinocyte cultures were strongly stained with anti-CGI-58 (**K**), anti-involucrin (**L**), and anti-transglutaminase 1 (**N**) antibodies, although only the upper layers were positive for loricrin (**M**). Immunofluorescent labeling and mRNA expression of each protein were consistent with each other: CGI-58 (**B**, **F**, **K**), involucrin (**C**, **G**, **L**), loricrin (**D**, **H**, **M**), transglutaminase 1 (**E**, **I**, **N**), green (FITC); nuclear stain, red (propidium iodide). Scale bars = 20 μ m.

CGI-58 Expression during Human Epidermal Development

In the two layered human fetal epidermis at 49 days EGA, weak CGI-58 immunostaining was seen in the epidermal cells (Figure 7A). In the three-layered human fetal epidermis at 76 days EGA, periderm cells were positive for CGI-58 (Figure 7B). In the four or more layered developing epidermis at 97 days and 105 days EGA, CGI-58 was expressed in the upper epidermis, predominantly in periderm cells (Figure 7, C and D). The upper epidermal cells, mainly the granular layer cells, were positive for CGI-58 in human fetal keratinized epidermis at 135 days EGA (Figure 7E). By this stage of development, periderm cells were already regressed.

We examined the expression of CGI-58 mRNA by real-time RT-polymerase chain reaction. The expression level of each mRNA was converted to a percentage rate compared to that of the normal adult skin (Figure 7F). CGI-58 mRNA was expressed in the early epidermal development at 10 weeks EGA (at 8.7% of adult expression level). At 15 weeks EGA, the CGI-58 mRNA expression level increased to 11.7% of adult level. The expression level of CGI-58 mRNA then markedly increased to 27.3% of adult levels at 18–20 weeks EGA when compared with an earlier developmental stage (10 and 15 weeks EGA). This increase in CGI-58 mRNA expression is consistent with CGI-58 immunofluorescence findings during human epidermal development. These results further support the idea that CGI-58 expression is up-regulated during keratinocyte differentiation.

Effect of Anti-CGI-58 MiRNA Silencing on the Expression of Keratinocyte Differentiation Markers

From the results described above, it was revealed that CGI-58 expression is up-regulated in accordance with expression of other keratinocyte differentiation markers. Thus, we studied the expression of keratinocyte differen-

tiation (keratinization) markers in CGI-58 knockdown keratinocytes to evaluate the effect of CGI-58 expression on the expression of keratinization markers.

For validation purposes, two different miRNAs (miRNA-CGI-58 #1 and #2) targeting different regions of human CGI-58 lacking homology to other human genomic sequences were used (see Materials and Methods for detail). A scrambled (random) non-targeting miRNA was used as negative control. Infection of normal human keratinocytes cultured in the high Ca²⁺ conditions with lentiviruses carrying miRNA targeting CGI-58 (miRNA-CGI-58 #1 and #2), but not lentiviruses containing scrambled, random negative control miRNA resulted in the effective knockdown of CGI-58 expression. The CGI-58 expression rates in the CGI-58 knockdown cells compared to control cells infected with a scrambled miRNA were 0.17 (miRNA-CGI-58 #1) and 0.12 (miRNA-CGI-58 #2) (Figure 8). We found that both the lentiviral vectors targeting different regions of CGI-58 mRNA had a sufficient ability to bring down CGI-58 expression in keratinocytes.

Notably, concomitant with decreases in CGI-58 expression, all of the four keratinization markers examined, involucrin, filaggrin, loricrin, and transglutaminase 1, showed a marked reduction in their mRNA expression levels. The expression rates of the differentiation markers in the CGI-58 knockdown cells compared to control cells were as follows: involucrin, 0.44 (miRNA-CGI-58 #1) and 0.46 (miRNA-CGI-58 #2); filaggrin, 0.18 (miRNA-CGI-58 #1) and 0.27 (miRNA-CGI-58 #2); loricrin, 0.18 (miRNA-CGI-58 #1) and 0.37 (miRNA-CGI-58 #2); and, transglutaminase 1, 0.54 (miRNA-CGI-58 #1) and 0.36 (miRNA-CGI-58 #2) (Figure 8). These results suggested that CGI-58 expression is crucial for the maintenance of expression of keratinization markers and for the normal keratinocyte differentiation process.

Discussion

In DCS patients, the amounts of triacylglycerol in lymphocytes, macrophages and fibroblasts cultured from patients were remarkably higher than those of normal controls.^{16,17} The causative defects in lipid metabolism in DCS patients are expected to involve triacylglycerol metabolism,¹⁸ especially in the catabolism of long-chain

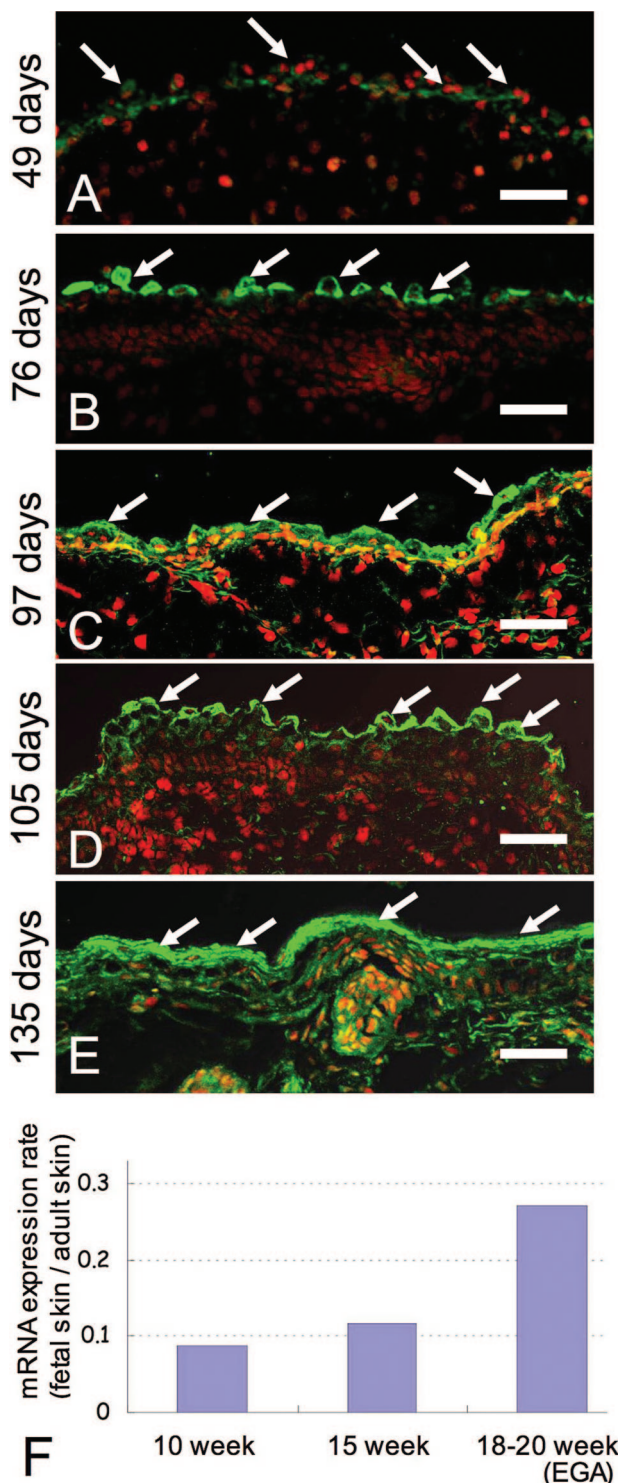


Figure 7. Expression of CGI-58 in developing human skin (A) in two-layered epidermis (at 49 days EGA), weak CGI-58 staining (green, FITC; **white arrows**) was seen in the epidermis; (B) in the three-layered epidermis (76 days EGA), CGI-58 staining was observed only in the periderm (**white arrows**). C, D: Non-keratinized four- or more-layered epidermis (C, 97 days EGA; D, 105 days EGA), CGI-58 immunolabeling was seen in the upper epidermis, mainly in the periderm (**white arrows**). E: in the keratinized fetal epidermis (135 days EGA), CGI-58 staining was seen in the upper epidermis, predominantly the granular layer (**white arrows**). CGI-58, green (FITC); nuclear stain, red (propidium iodide). Scale bars = 50 μ m. F: Expression of CGI-58 mRNA was up-regulated during human fetal skin development. The mRNA expression levels (fetal skin/adult skin) were summarized in the graph. At 18 and 20 weeks EGA, the rate of CGI-58 mRNA expression was significantly increased and reached approximately 0.27 compared to adult skin levels. Immunofluorescent labeling and mRNA expression levels were consistent with each other.

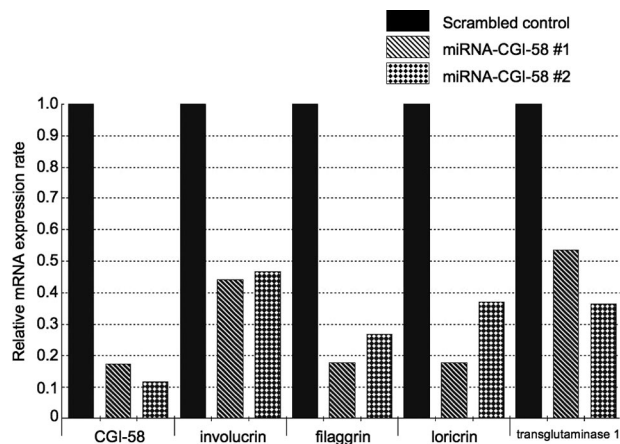


Figure 8. Lentiviral-Mediated Knockdown of CGI-58 Expression in Cultures of Human Keratinocytes. Two lentiviruses targeting different regions of CGI-58 (miRNA-CGI-58 #1 and miRNA-CGI-58 #2) showed similar depletion/knockdown of CGI-58 mRNA expression. Expression of keratinization markers, involucrin, filaggrin, loricrin, and transglutaminase 1, was markedly reduced after infection with lentiviruses carrying miRNA-CGI-58 #1 and miRNA-CGI-58 #2 constructs.

fatty acids^{17,19} or in the recycling pathway involving triacylglycerol-derived mono- or diacylglycerol conversion into phospholipids.^{20,21} Thus, once CGI-58 was identified as a causative molecule for DCS,^{3,4} speculation has arisen that CGI-58 plays an important role in triacylglycerol metabolism in several organs including the skin.

CGI-58 belongs to a large family of proteins characterized by an α/β -fold domain^{22,23} and comprise a catalytic triad composed of a nucleophile, an acidic domain and histidine.^{24,25} From analysis of the reported amino acid sequences, we know that CGI-58 has a putative catalytic triad similar to other members of the esterase/lipase/thioesterase subfamily.³ CGI-58 was reported to localize to lipid droplets.²⁶ Adipose triglyceride lipase was recently identified as an important triacylglycerol hydrolase promoting the catabolism of stored fat in adipose and nonadipose tissues.² It was demonstrated that efficient adipose triglyceride lipase enzyme activity requires activation by CGI-58.² CGI-58 interacts with adipose triglyceride lipase, stimulating its triacylglycerol hydrolase activity by up to 20-fold.² Antisense RNA-mediated reduction of CGI-58 expression in 3T3-L1 adipocytes inhibits triacylglycerol mobilization.² Furthermore, expression of functional CGI-58 in DCS fibroblasts restores lipolysis and reverses the abnormal triacylglycerol accumulation typical for DCS.² These facts suggest an important biochemical function for CGI-58 in the lipolytic degradation of fat.²

The precise pathomechanisms of CGI-58 mutations causing multiorgan symptoms in DCS, particularly liver dysfunction and mental retardation, remains to be clarified. From our results, CGI-58 is expressed in the cytoplasm of hepatocytes, medium sized multipolar neurons in the hypothalamus, corneal epithelial cells and dermal fibroblasts. LGs or any equivalent organ specific variant of LGs has not been reported in these cells. In hepatocytes, CGI-58 expression might be associated with lipid droplets or peroxisomes. CGI-58 expression in hepatocytes and neurons is probably related to liver dysfunction

and a variety of DCS neurological symptoms respectively. We could not obtain any further clues to clarify a role of CGI-58 in dermal fibroblasts in the present study.

As for lipid metabolism in the skin, intercellular lipid layers are crucial for barrier function of the human epidermis.¹² All ceramides, cholesterol, and free fatty acids are essential elements for the normal intercellular lipid layers.¹²

Epidermal keratinocyte LGs are multifunctional as they package and secrete a variety of enzymes and structural proteins. One of their important functions is lipid transport and secretion for the formation of the intercellular stratum corneum lipid layers. Formation of a normal epidermal permeability barrier and normal desquamation require the active secretion of LG contents into the intercellular spaces between the granular and cornified cells. LGs contain both polar lipids and various hydrolytic enzymes that catalyze the extracellular processing of the secreted polar lipids into more hydrophobic reaction products.²⁷

In the present study, we clearly demonstrated that CGI-58 is located in epidermal keratinocyte LGs. Remarkably reduced CGI-58 immunostaining was observed in LG deficient harlequin ichthyosis epidermis and further confirmed the localization of CGI-58 in LGs. The unaltered distribution of the LG-non-lipid content together with a TGN marker was observed in the CGI-58-null epidermis.

In previous studies, ultrastructurally abnormal LGs containing irregularly-shaped granular or vesicular material were observed within the granular layer cells of CGI-58 null epidermis.⁴ Elias and Williams²⁸ also reported an abnormality in the lipid content of LGs in multiple DCS cases from a single family, although the underlying mutations from the family had not been detected. Recently, skin barrier dysfunction was confirmed in DCS patients.²⁹

Abnormal LGs and an abnormal transport of LG contents are frequently reported as the main pathomechanisms for other congenital ichthyoses including harlequin ichthyosis.¹³ In harlequin ichthyosis, LGs are absent or, if present, they show an abnormal empty or vesiculated content without any lamellar structure. These abnormal LGs are not secreted to the intercellular space and they accumulate to form a large number of lipid droplets within the cornified cells.³⁰⁻³² These severe abnormalities were identified as due to a deficiency in the keratinocyte lipid transporter ABCA12.¹³ In contrast, a functional TGN and LG system is formed in cases with DCS and LG contents are secreted to the intercellular space. These differences in LG abnormalities are probably due to the differing roles of CGI-58 and ABCA12 in lipid transport and metabolism in keratinocytes. Taking all these facts and data from the present study into consideration, we conclude that CGI-58 localizes to the lipid transporting LGs and is up-regulated during keratinization. Triacylglycerols have been suggested as a precursor pool for sphingolipids,^{33,34} although LGs are not known to contain triacylglycerols.³⁵ CGI-58 is known to stimulate triacylglycerol hydrolase activity, though CGI-58 itself does not have lipase activity.² Thus, there is a possibility that CGI-58 is associated with synthesis of sphingolipids that

are essential for the stratum corneum lipid barrier. In DCS patients, CGI-58 deficiency is thought to result in defective skin lipid barrier formation leading to an ichthyotic phenotype.

Furthermore, in the present study, CGI-58 expression in cultured keratinocytes was mildly up-regulated in high Ca²⁺ culture conditions and was remarkably up-regulated in three-dimensional, organotypic cultures. These findings apparently indicate that keratinocyte CGI-58 expression is up-regulated by keratinocyte differentiation (keratinization). During human fetal skin development, CGI-58 was expressed in the periderm of three layered epidermis from the early fetal period and, in the later stages of fetal skin development, CGI-58 expression was mainly seen in the upper epidermis, similar to the CGI-58 distribution in adult epidermis. This pattern of developmental expression was similar to other keratinization-associated molecules, such as transglutaminase 1 and ABCA12.^{15,36,37} To further clarify the functional role of CGI-58 during normal human keratinocyte differentiation, we performed knockdown of CGI-58 expression using an RNAi approach, in which we used short RNA duplex-containing sequences complementary to CGI-58 mRNA to induce specific inhibition of its expression. CGI-58 knockdown led to reduced expression of all of the keratinocyte differentiation markers examined, ie, involucrin, loricrin, filaggrin, and transglutaminase 1. These results suggest that CGI-58 might be important for keratinocyte differentiation (keratinization) process. In conclusion, we considered that CGI-58 is packed in LGs and is likely associated with intercellular lipid layer formation in the stratum corneum and may play a crucial role in keratinocyte differentiation and keratinization.

Acknowledgments

We thank Dr. Yoshikazu Uchida for his helpful discussion, Mrs. Megumi Sato, Dr. Maki Goto, and Ms. Akari Nagasaki for their technical assistance.

References

- Lai CH, Chou CY, Ch'ang LY, Liu CS, Lin W: Identification of novel human genes evolutionarily conserved in *Caenorhabditis elegans* by comparative proteomics. *Genome Res* 2000, 10:703-713
- Lass A, Zimmermann R, Haemmerle G, Riederer M, Schoiswohl G, Schweiger M, Kienesberger P, Strauss JG, Gorkiewicz G, Zechner R: Adipose triglyceride lipase-mediated lipolysis of cellular fat stores is activated by CGI-58 and defective in Chanarin-Dorfman syndrome. *Cell Metab* 2006, 3:309-319
- Lefèvre C, Jobard F, Caux F, Bouadjar B, Karaduman A, Heilig R, Lakhdar H, Wollenberg A, Verret JL, Weissenbach J, Ozguc M, Lathrop M, Prud'homme JF, Fischer J: Mutations in CGI-58, the gene encoding a new protein of the esterase/lipase/thioesterase subfamily, in Chanarin-Dorfman syndrome. *Am J Hum Genet* 2001, 69:1002-1012
- Akiyama M, Sawamura D, Nomura Y, Sugawara M, Shimizu H: Truncation of CGI-58 protein causes malformation of lamellar granules resulting in ichthyosis in Dorfman-Chanarin syndrome. *J Invest Dermatol* 2003, 121:1029-1034
- Caux F, Selma ZB, Laroche L, Prud'homme JF, Fischer J: CGI-58/ABHD5 gene is mutated in Dorfman-Chanarin syndrome. *Am J Med Genet A* 2004, 129:214
- Schleinitz N, Fischer J, Sanchez A, Veit V, Harle JR, Pelissier JF: Two new mutations of the ABHD5 gene in a new adult case of Chanarin Dorfman syndrome: an uncommon lipid storage disease. *Arch Dermatol* 2005, 141:798-800
- Pujol RM, Gilaberte M, Toll A, Florensa L, Lloreta J, Gonzalez-Ensenat MA, Fischer J, Azon A: Erythrokeratoderma variabilis-like ichthyosis in Chanarin-Dorfman syndrome. *Br J Dermatol* 2005, 153:838-841
- Dorfman ML, Hershko C, Eisenberg S, Sagher F: Ichthyosiform dermatosis with systemic lipidosis. *Arch Dermatol* 1974, 110:261-266
- Chanarin I, Patel A, Slavin G, Wills EJ, Andrews TM, Stewart G: Neutral-lipid storage disease: a new disorder of lipid metabolism. *Br Med J* 1975, 1:553-555
- Williams MLK, Lynch PJ: Generalized disorders of cornification: The ichthyoses. *Principles and Practice of Dermatology*, Second Edition, Edited by WM Sams Jr, Lynch PJ. New York, Churchill Livingstone, 1996. pp. 379-396
- Pena-Penabad C, Almagro M, Martinez W, Garcia-Silva J, Del Pozo J, Yebra MT, Sanchez-Manzano C, Fonseca E: Dorfman-Chanarin syndrome (neutral lipid storage disease): new clinical features. *Br J Dermatol* 2001, 144:430-432
- Elias PM: Stratum corneum defensive functions: an integrated view. *J Invest Dermatol* 2005, 125:183-200
- Akiyama M, Sugiyama-Nakagiri Y, Sakai K, McMillan JR, Goto M, Arita K, Tsuji-Abe Y, Tabata N, Matsuoka K, Sasaki R, Sawamura D, Shimizu H: Mutations in lipid transporter ABCA12 in harlequin ichthyosis and functional recovery by corrective gene transfer. *J Clin Invest* 2005, 115:1777-1784
- Sawamura D, Goto M, Shibaki A, Akiyama M, McMillan JR, Abiko Y, Shimizu H: Beta defensin-3 engineered epidermis shows highly protective effect for bacterial infection. *Gene Ther* 2005, 12:857-861
- Akiyama M, Smith LT, Yoneda K, Holbrook KA, Hohl D, Shimizu H: Periderm cells form cornified cell envelope in their regression process during human epidermal development. *J Invest Dermatol* 1999, 112:903-909
- Williams ML, Monger DJ, Rutherford SL, Hincenbergs M, Rehfeld SJ, Grunfeld C: Neutral lipid storage disease with ichthyosis: lipid content and metabolism of fibroblasts. *J Inher Metab Dis* 1988, 11:131-143
- Hilaire N, Salvayre R, Thiers JC, Bonnafé MJ, Nègre-Salvayre A: The turnover of cytoplasmic triacylglycerols in human fibroblasts involves two separate acyl chain length-dependent degradation pathways. *J Biol Chem* 1995, 270:27027-27034
- Williams ML, Coleman RA, Placezk D, Grunfeld C: Neutral lipid storage disease: a possible functional defect in phospholipid-linked triacylglycerol metabolism. *Biochim Biophys Acta* 1991, 1096:162-169
- Hilaire N, Nègre-Salvayre A, Salvayre R: Cellular uptake and catabolism of high-density-lipoprotein triacylglycerol in human cultured fibroblasts: degradation block in neutral lipid storage disease. *Biochem J* 1994, 297:467-473
- Igal RA, Coleman RA: Acylglycerol recycling from triacylglycerol to phospholipid, not lipase activity, is defective in neutral lipid storage disease fibroblasts. *J Biol Chem* 1996, 271:16644-16651
- Igal RA, Coleman RA: Neutral lipid storage disease: a genetic disorder with abnormalities in the regulation of phospholipid metabolism. *J Lipid Res* 1998, 39:31-43
- Ollis DL, Cheah E, Cygler M, Dijkstra B, Frolow F, Franken SM, Harel M, Remington SJ, Silman I, Schrag J, Sussman JL, Verschuuren KHG, Goldman A: The alpha/beta hydrolase fold. *Protein Eng* 1992, 5:197-211
- Heikinheimo P, Goldman A, Jeffries C, Ollis DL: Of barn owls and bankers: a lush variety of alpha/beta hydrolases. *Struct Fold Des* 1997, R141-R146
- Zhang L, Godzik A, Skolnick J, Fetrow JS: Functional analysis of the *Escherichia coli* genome for members of the alpha/beta hydrolase family. *Fold Des* 1998, 3:535-548
- Nardini M, Dijkstra BW: alpha/beta Hydrolase fold enzymes: the family keeps growing. *Curr Opin Struct Biol* 1999, 9:732-737
- Yamaguchi T, Omatsu N, Matsushita S, Osumi T: CGI-58 interacts with perlipin and is localized to lipid droplets. Possible involvement of CGI-58 mislocalization in Chanarin-Dorfman syndrome. *J Biol Chem* 2004, 279:30490-30497
- Rassner U, Feingold KR, Crumrine DA, Elias PM: Coordinate assembly of lipids and enzyme proteins into epidermal lamellar bodies. *Tissue Cell* 1999, 31:489-498
- Elias PM, Williams ML: Neutral lipid storage disease with ichthyosis.

- Defective lamellar body contents and intracellular dispersion. *Arch Dermatol* 1985, 121:1000–1008
29. Demerjian M, Crumrine DA, Milstone LM, Williams ML, Elias PM: Barrier dysfunction and pathogenesis of neutral lipid storage disease with ichthyosis (Chanarin-Dorfman syndrome). *J Invest Dermatol* 2006, 126:2032–2038
 30. Dale BA, Holbrook KA, Fleckman P, Kimball JR, Brumbaugh S, Sybert VP: Heterogeneity in harlequin ichthyosis, an inborn error of epidermal keratinization: variable morphology and structural protein expression and a defect in lamellar granules. *J Invest Dermatol* 1990, 94:6–18
 31. Milner ME, O'Guin WM, Holbrook KA, Dale BA: Abnormal lamellar granules in harlequin ichthyosis. *J Invest Dermatol* 1992, 99:824–829
 32. Akiyama M, Kim D-K, Main DM, Otto CE, Holbrook KA: Characteristic morphological abnormality of harlequin ichthyosis detected in amniotic fluid cells. *J Invest Dermatol* 1994, 102:210–213
 33. Madison KC, Swartzendruber DC, Wertz PW, Downing DT: Murine keratinocyte cultures grown at the air/medium interface synthesize stratum corneum lipids and "recycle" linoleate during differentiation. *J Invest Dermatol* 1989, 93:10–17
 34. Wertz PW, Downing DT: Metabolism of linoleic acid in porcine epidermis. *J Lipid Res* 1990, 31:1839–1844
 35. Grayson S, Johnson-Winegar AG, Wintroub BU, Isseroff RR, Epstein EH Jr., Elias PM: Lamellar body-enriched fractions from neonatal mice: preparative techniques and partial characterization. *J Invest Dermatol* 1985, 85:289–294
 36. Akiyama M, Smith LT, Shimizu H: Expression of transglutaminase activity in developing human epidermis. *Br J Dermatol* 2000, 142:223–225
 37. Yamanaka Y, Akiyama M, Sugiyama-Nakagiri Y, Sakai K, Goto M, McMillan JR, Ota M, Sawamura D, Shimizu H: Expression of the keratinocyte lipid transporter ABCA12 in developing and reconstituted human epidermis. *Am J Pathol* 2007, 171:43–52